THE JOURNAL OF BIOLOGICAL CHEMISTRY VOL. 281, NO. 42, pp. 31659–31667, October 20, 2006

The Reactions of Heme- and Verdoheme-Heme Oxygenase-1 Complexes with FMN-depleted NADPH-cytochrome P450 Reductase

ELECTRONS REQUIRED FOR VERDOHEME OXIDATION CAN BE TRANSFERRED THROUGH A PATHWAY NOT INVOLVING FMN[*S]

Received for publication, June 28, 2006, and in revised form, August 11, 2006 Published, JBC Papers in Press, August 22, 2006, DOI 10.1074/jbc.M606163200

Yuichiro Higashimoto[‡1,2], Hideaki Sato[‡1], Hiroshi Sakamoto[§], Kenichi Takahashi[‡], Graham Palmer[¶], and Masato Noguchi[‡3]

From the [‡]Department of Medical Biochemistry, Kurume University School of Medicine, Kurume 830-0011, Japan, the [§]Department of Bioscience and Bioinformatics, Kyushu Institute of Technology, Iizuka 820-8502, Japan, and the [¶]Department of Biochemistry and Cell Biology, Rice University, Houston, Texas 77005-1892

Electrons utilized in the heme oxygenase (HO) reaction are provided by NADPH-cytochrome P450 reductase (CPR). To investigate the electron transfer pathway from CPR to HO, we examined the reactions of heme and verdoheme, the second intermediate in the heme degradation, complexed with rat HO-1 (rHO-1) using a rat FMN-depleted CPR; the FMN-depleted CPR was prepared by dialyzing the CPR mutant, Y140A/Y178A, against 2 M KBr. Degradation of heme in complex with rHO-1 did not occur with FMN-depleted CPR, notwithstanding that the FMN-depleted CPR was able to associate with the heme-rHO-1 complex with a binding affinity comparable with that of the wild-type CPR. Thus, the first electron to reduce the ferric iron of heme complexed with rHO-1 must be transferred from FMN. In contrast, verdoheme was converted to the ferric biliverdin-iron chelate with FMN-depleted CPR, and this conversion was inhibited by ferricyanide, indicating that electrons are certainly required for conversion of verdoheme to a ferric biliverdin-iron chelate and that they can be supplied from the FMN-depleted CPR through a pathway not involving FMN, probably via FAD. This conclusion was supported by the observation that verdoheme dimethyl esters were accumulated in the reaction of the ferriprotoporphyrin IX dimethyl ester-rHO-1 complex with the wild-type CPR. Ferric biliverdin-iron chelate, generated with the FMN-depleted CPR, was converted to biliverdin by the addition of the wild-type CPR or desferrioxamine. Thus, the final electron for reducing ferric biliverdin-iron chelate to release ferrous iron and biliverdin is apparently provided by the FMN of CPR.

Heme oxygenase (HO[4]; EC 1.14.99.3) is a microsomal enzyme that catalyzes the degradation of heme to biliverdin IXα, carbon monoxide (CO), and free iron in the presence of NADPH-cytochrome P450 reductase (CPR; EC 1.6.2.4) (1–3). The HO reaction proceeds via a multistep mechanism as shown in Fig. 1 (4, 5). The first step is the oxidation of heme to α-hydroxyheme, requiring molecular oxygen (O_2) and reducing equivalents supplied by CPR (6–8). The second step is the formation of verdoheme with the concomitant release of hydroxylated α-*meso* carbon as CO (9–11). The third step is the conversion of α-verdoheme to a biliverdin-iron chelate, for which O_2 and electrons from CPR are also required (12). In the last step, the iron of the biliverdin-iron chelate is reduced, and finally ferrous iron and biliverdin are released from HO. The conversion of verdoheme to the ferric biliverdin-iron chelate along with the release of biliverdin is a rate-limiting step in the HO reaction (13). The mechanism of degradation of verdoheme is the least understood of the three successive oxygenation reactions during the HO catalysis, although some chemical mechanisms have been proposed (12, 14).

CPR is an FAD- and FMN-containing protein that supplies electrons required for the HO reaction as well as for a variety of other hemoproteins, such as cytochrome P450s and cytochrome b_5. With the latter hemoproteins, it is thought that electrons from NADPH flow first to FAD and then to FMN and finally to their heme groups (15–17). For electron transfer, CPR and its redox partners need to associate with each other. Indeed, the molecular surface of HO-1 surrounding the exposed δ-*meso* edge of heme is positively charged and can form an electrostatic complex with the negatively charged surface of CPR (18).

* This work was supported in part by Grants-in-Aid for Young Scientists 18770121 (to Y. H.) and 17750164 (to H. Sato) from the Ministry of Education, Culture, Sports, Science, and Technology of Japan, by Grants-in-Aid for Scientific Research 18590278 (to M. N.) and 18550153 (to H. Sakamoto) from the Japan Society for the Promotion of Science, by National Institutes of Health Grant GM 55807 (to G. P.), by a grant from the Samurou Kakiuchi Foundation for the Promotion of Science (to H. Sakamoto), and by a grant from the Morikazu Kaibara Medical Science Promotion Foundation (to Y. H.). The costs of publication of this article were defrayed in part by the payment of page charges. This article must therefore be hereby marked "*advertisement*" in accordance with 18 U.S.C. Section 1734 solely to indicate this fact.

[S] The on-line version of this article (available at http://www.jbc.org) contains supplemental Figs. S1–S4 and Tables S1 and S2.

[1] These authors contributed equally to this work.

[2] To whom correspondence may be addressed. Tel.: 81-942-31-7544; Fax: 81-942-31-4377; E-mail: higashiy@med.kurume-u.ac.jp.

[3] To whom correspondence may be addressed. Tel.: 81-942-31-7544; Fax: 81-942-31-4377; E-mail: mnoguchi@med.kurume-u.ac.jp.

[4] The abbreviations used are: HO, heme oxygenase; rHO-1, a soluble form of rat HO-1 lacking the 22-amino acid C-terminal hydrophobic segment; CPR, NADPH-cytochrome P450 reductase; heme, iron protoporphyrin IX, either ferrous or ferric form; FePPDME, iron protoporphyrin IX dimethyl ester, either ferrous or ferric form; HPLC, high pressure liquid chromatography.

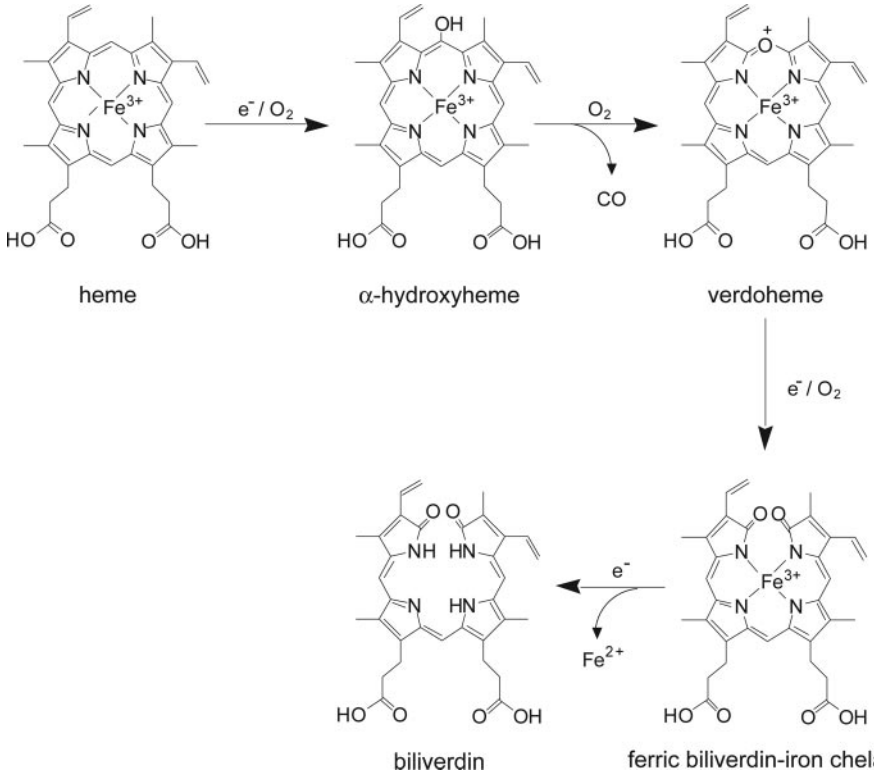

FIGURE 1. **Oxidative degradation of heme catalyzed by HO.** HO catalyzes the degradation of heme to biliverdin IXα through three distinct intermediates, α-hydroxyheme, α-verdoheme, and biliverdin-iron chelate, at the expense of O_2 and reducing equivalents.

Recently, using site-specific mutation and docking modeling, we have found that Arg^{185} and Lys^{149} of rat HO-1 (rHO-1) are important in both the HO activity and its association with CPR (19). In our model, the guanidino group of Arg^{185} interacts electrostatically with 2′-phosphate of NADPH in CPR, whereas Lys^{149} is close to a cluster of acidic amino acids near the FMN binding site of CPR (Fig. 2). Thus, Arg^{185} and Lys^{149} appear to interact with CPR in such a way as to orient the redox partners for optimal electron transfer from the FMN of CPR to the heme of HO-1. The model also suggested that the electrons from CPR are transferred through the distal side of the heme pocket to heme and that Lys^{149} is involved in the electron transfer from FMN. However, Arg^{185} appeared not to be involved in electron transfer from FMN, since its location is far from the FMN binding site of CPR.

Thus far, crystal structures of rat and/or human HO-1 in the heme-free (20, 21), heme-bound (22, 23), verdoheme-bound (14), biliverdin-iron chelate-bound (24), and biliverdin-bound forms (25) have been reported. In particular, the crystal structure of the heme-bound form (heme-HO-1 complex) revealed that the highly conserved Lys^{179} and Arg^{183} residues interact electrostatically with the heme propionate groups and that these residues play important roles in the α-regiospecificity of HO catalysis (22, 23, 26). The necessity of the heme propionate side chains at the C-6 and C-7 positions for the HO reaction has been also suggested from previous studies on the substrate specificity of HO using a variety of modified hemes (27, 28). Specifically, a modified heme, in which the C-6 and C-7 propionates are substituted with butyrates, can be degraded to bilirubin at only half the rate observed with the normal heme under the usual HO reaction conditions containing CPR and biliverdin reductase, whereas the heme modified with acetates cannot serve as a substrate for HO. Furthermore, it has been shown that the catalytic activity of the R183E mutant of human HO-1 was decreased to only 2–3% that of the wild-type enzyme in the NADPH/CPR-supported reaction (yielding 100% of α-isomer), whereas no significant decrease of activity was observed in the ascorbate-supported reaction (yielding 80% α-isomer and 20% δ-isomer) (29, 30). In parallel with this, the electron transfer rate from CPR was drastically decreased with the R183E mutant (31). These facts suggest that the electrostatic interaction between Arg^{183} of HO and the heme propionates may play an important role not only in the α-regiospecificity of the HO catalysis but also in electron transfer between CPR and HO.

In order to shed light on the electron transfer mechanism from CPR to HO and also to explore how the interactions between the basic residues, Lys^{179} and Arg^{183}, and the heme propionates are involved in the electron transfer, we prepared a rat FMN-depleted CPR and compared the degradation of heme, verdoheme, and ferriprotoporphyrin IX dimethyl ester (FePPDME) complexed with rHO-1 using the wild-type CPR and the FMN-depleted CPR. Here we present evidence that the FMN-depleted CPR can support the conversion of verdoheme to the ferric biliverdin-iron chelate, indicating that electrons required for verdoheme oxidation can be transferred through a pathway not involving FMN.

EXPERIMENTAL PROCEDURES

Materials—FAD, NADPH, hemin, hexafluoroacetone, desferrioxamine, potassium ferricyanide, and cytochrome *c* were purchased from Sigma; FMN and sodium ascorbate were from Nacalai Tesque (Kyoto, Japan); and FePPDME was from Frontier Scientific (Logan, UT). By matrix-assisted laser desorption/ionization time-of-flight mass spectrometry analysis, it was confirmed that the FePPDME (*m/z* 644.4 found, 644.2 calc) did not contain unesterified hemin. α-Verdoheme (hereafter referred to as verdoheme) was synthesized and purified as reported earlier (10). Formation of verdoheme was confirmed by its optical absorption spectrum (λ_{max} in aqueous pyridine solution: 397, 505, 534, and 680 nm). Concentration of the bispyridine complex of verdoheme was determined spectrophotometrically using $\epsilon_{397} = 53.3\ mM^{-1}\ cm^{-1}$ (10). All spectrophotometric analyses were conducted on a Varian Cary 50 Bio UV-visible spectrophotometer at room temperature or at the temperatures indicated.

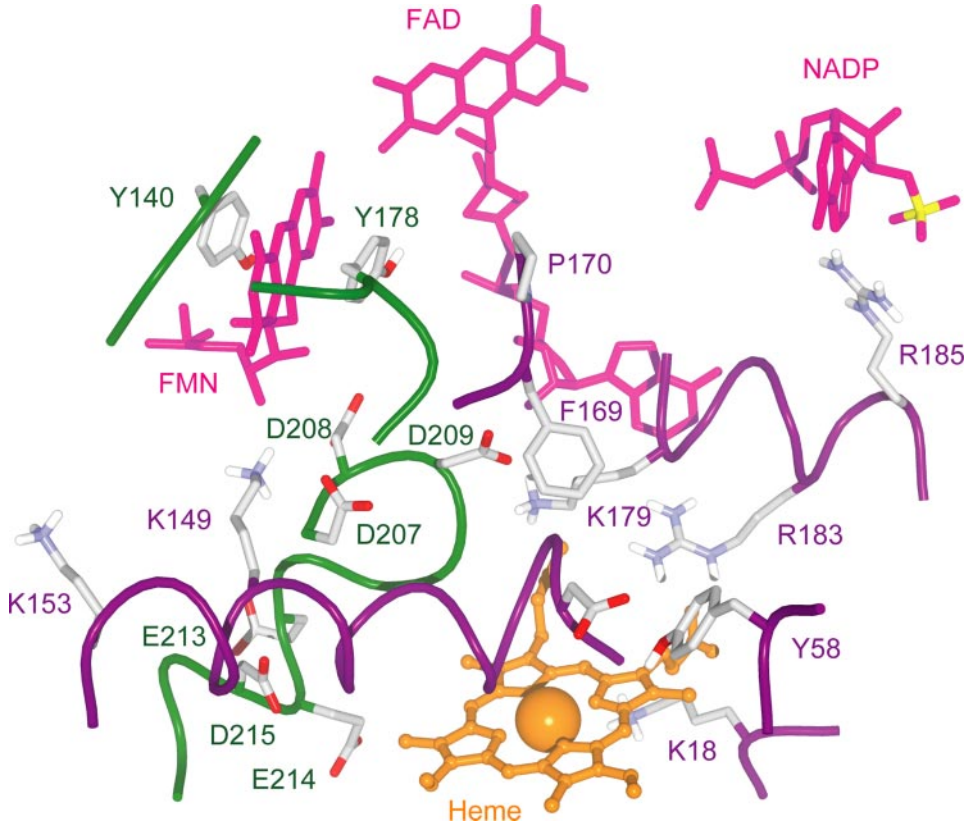

FIGURE 2. **Diagram of the critical amino acids surrounding the cofactor binding sites at the interface between CPR and the heme-rHO-1 complex (19).** HO-1 and CPR are represented as *purple-* and *green-colored tubes*, respectively. The side chains of residues are shown as *sticks* (carbon in *white*, oxygen in *red*, and nitrogen in *light blue*). NADP (phosphorus in *yellow*), FAD, and FMN are shown by *magenta sticks*, and heme is shown by the *ball-and-sticks* (*orange*).

Preparation of Heme-rHO-1, Verdoheme-rHO-1, and FePPDME-rHO-1 Complexes—A soluble form of rHO-1 lacking the 22-amino acid C-terminal hydrophobic segment was expressed in *Escherichia coli* and purified as described previously (32). The ferric heme complex of rHO-1 was reconstituted with 1.2 eq of heme and purified by column chromatography on hydroxyapatite (Bio-Rad) as previously described (32).

The reconstitution and purification of the verdoheme-rHO-1 complex were performed as reported previously (10). Briefly, to the rHO-1 solution (~0.1 mM) in 0.1 M potassium phosphate, pH 7.4, was added a slight excess of verdoheme as an aqueous pyridine solution. The mixture was incubated at 4 °C for 1 h and then passed through a Sephadex G-25 gel filtration column. The purified ferrous verdoheme-rHO-1 complex exhibited absorption maxima at 399 nm ($\epsilon = 50.2\ mM^{-1}\ cm^{-1}$) and 534 and 688 nm with an $A_{399\ nm}/A_{280\ nm}$ value of 1.1 (12).

The reconstitution and purification of the FePPDME-rHO-1 complex were carried out in a similar manner. To the rHO-1 solution (~1 μM) in 0.1 M potassium phosphate, pH 7.4, was added a slight excess of FePPDME dissolved in pyridine. The mixture was kept on ice for 30 min, and the FePPDME·rHO-1 complex was purified by column chromatography on hydroxyapatite. Fractions containing the complex were pooled and concentrated by ultrafiltration. The approximate concentration of FePPDME-rHO-1 complex was estimated employing $\epsilon = 140\ mM^{-1}\ cm^{-1}$ of the Soret band of ferric heme-rHO-1 complex (33).

Preparation of Wild-type CPR and Its Y140A/Y178A Mutant—A recombinant rat liver CPR lacking the N-terminal 57 hydrophobic amino acids, called wild-type CPR in this study, was expressed and purified as previously described (34). The CPR mutant, Y140A/Y178A, was generated from the wild type with the Stratagene QuikChange site-directed mutagenesis kit (Stratagene, La Jolla, CA). The mutations were confirmed by DNA sequencing. The homogeneity of the purified enzymes was determined by SDS-PAGE.

Preparation and Characterization of FMN-depleted CPR—FMN-depleted CPR was prepared from the Y140A/Y178A mutant, taking advantage of the KBr method reported in Ref. 35. The Y140A/Y178A mutant was dialyzed overnight, with one change of the buffer solution, against 2 M KBr in 0.05 M potassium pyrophosphate buffer, pH 8.5, containing 10% glycerol. The KBr-treated mutant was then dialyzed overnight against 0.02 M potassium phosphate buffer, pH 7.7, to remove the KBr. The flavin contents in CPR were determined by HPLC with minor modifications of the procedure of Kurzban and Strobel (36). The reductase was denatured by dilution into 3 volumes of saturated guanidine hydrochloride. HPLC was carried out on a Waters model 600E multisolvent delivery system equipped with a Waters 996 photodiode array detector, a Waters 776 auto sampler, and Millennium software (Millipore Corp., Bedford, MA). A 5C18-MS-II (4.6 × 250 mm) column obtained from Nacalai Tesque was used. Elution was conducted using a 40-ml linear gradient from water containing 0.05% trifluoroacetic acid to acetonitrile containing 0.04% trifluoroacetic acid at a flow rate of 1 ml/min and was monitored at 450 nm. Flavines were quantified by peak area based on the standard curves constructed with authentic FAD or FMN.

Measurement of cytochrome *c*-reducing activity of CPR was carried out at 28 °C with a reaction mixture of 0.27 M potassium phosphate, pH 7.7, 50 μM NADPH, and 65 μM cytochrome *c* in a final volume of 1.0 ml (37). The ferricyanide-reducing activity of CPR was measured at 28 °C with a reaction mixture of 0.3 M potassium phosphate, pH 7.7, 100 μM NADPH, and 500 μM potassium ferricyanide in a final volume of 1.0 ml (36). The binding affinity of the heme-rHO-1 complex with CPR was determined by surface plasmon resonance technology using a BIAcore 1000 instrument (BIAcore AB, Uppsala, Sweden), as described previously (19).

TABLE 1

Quantification of the flavin contents of wild-type CPR and its mutant by HPLC

CPR	FMN	FAD
	mol/mol protein	
Wild-type CPR	1.12	0.90
Y140A/Y178A mutant	0.09	0.87
FMN-depleted CPR[a]	<0.004	0.85

[a] FMN-depleted CPR was prepared by dialyzing Y140A/Y178A mutant against 2 M KBr as described under "Experimental Procedures."

Single Turnover HO Reaction of Heme-rHO-1, Verdoheme-rHO-1, and FePPDME-rHO-1 Complexes—All single turnover reactions were monitored by optical absorption changes at 25 °C. Unless otherwise indicated, the reaction mixtures (0.1 ml) consisted of 5 μM heme-, verdoheme-, or FePPDME-rHO-1 complex, a 0.04–0.4 μM concentration of the wild-type or FMN-depleted CPR, and 25 μM NADPH in 0.1 M potassium phosphate buffer, pH 7.4. Spectra were recorded over the range of 300–900 nm. When ascorbate was employed as the reductant, 20 mM sodium ascorbate was added in place of the NADPH/CPR system. The effect of ferricyanide on the single turnover reaction of the verdoheme-rHO-1 complex (5 μM) was examined with the NADPH (25 μM)/FMN-depleted CPR (100 nM) system in the presence of ferricyanide (0–100 μM). Biliverdin dimethyl ester isomers produced in the single turnover reaction of FePPDME·rHO-1 complex were analyzed by HPLC as described previously (10).

RESULTS

Preparation and Characterization of FMN-depleted CPR—We first tried to prepare an FMN-free CPR by introducing a double mutation at Tyr^{140} and Tyr^{178}; these Tyr residues are known to be responsible for the binding of FMN to CPR (18, 37). Table 1 shows that the replacement of the two Tyr residues with Ala selectively decreased the FMN content from 1.12 to 0.09 mol/mol of protein, whereas no significant effect on the FAD content was detected. Dialysis against 2 M KBr (35, 38) resulted in thorough removal of FMN from the CPR mutant without affecting the FAD content. Hereafter, the KBr-treated mutant CPR will be referred to as the FMN-depleted CPR. CD analysis revealed that the spectrum of the FMN-depleted CPR was almost identical to that of the wild-type CPR, indicating that the deletion of FMN produced almost no effect on the CPR conformation (supplemental Table S1 and Fig. S1).

We next evaluated the electron transfer activities of the wild-type and the FMN-depleted CPR using cytochrome *c* and potassium ferricyanide as electron acceptors. As shown in Table 2, the wild-type CPR reduced cytochrome *c* and ferricyanide at rates of 54.8 and 66.7 μmol/min/mg protein, respectively. On the other hand, the FMN-depleted CPR almost completely lost the ability to transfer an electron to cytochrome *c* but retained ferricyanide reducing activity comparable with that of the wild-type CPR. These results are consistent with previous studies using the FMN-deficient CPRs that were prepared from the wild-type CPR by the KBr treatment (35, 36, 39). The possibility that removal of FMN from CPR would cause a decrease in the binding affinity of CPR for rHO-1 was ruled out by a surface plasmon resonance analysis; the dissociation constant for binding of heme-rHO-1 complex to the FMN-depleted CPR in the presence of $NADP^+$ was 0.44 ± 0.1 μM, which was comparable with that for the wild-type CPR (0.49 ± 0.1 μM (19)). Thus, the electron transfer activities of the FMN-depleted CPR are directly related to its flavin composition.

TABLE 2

Electron transfer activities of wild-type and FMN-depleted CPR

The assay conditions are described under "Experimental Procedures." The values of mean ± S.D. of three independent assays are presented.

Enzyme	Cytochrome *c*	Ferricyanide
	μmol/min/mg protein	
Wild-type CPR	54.8 ± 6.0	66.7 ± 6.8
FMN-depleted CPR	0.05 ± 0.02	62.4 ± 7.2

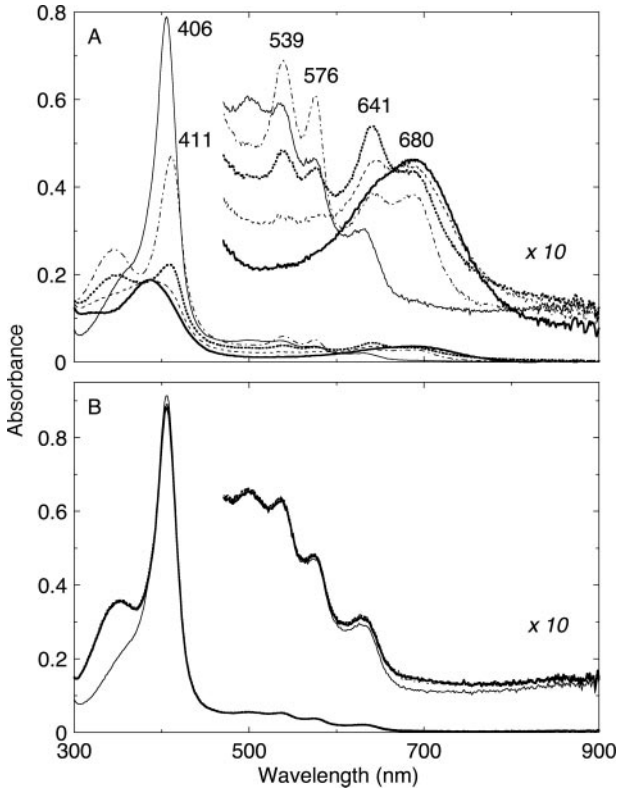

FIGURE 3. **Absorption spectral changes of the heme-rHO-1 complex during the NADPH/CPR-supported single turnover reaction.** The spectra were recorded before (*thin solid line*) and after the addition of NADPH (*dashed and dotted line*, 1 min; *dotted line*, 5 min; *dashed line*, 10 min; *thick solid line*, 25 min). The procedures are described under "Experimental Procedures." *A*, with wild-type CPR; *B*, with FMN-depleted CPR.

Single Turnover Reactions of Heme-rHO-1 Complex with NADPH/Wild-type and FMN-depleted CPR Systems—We first examined the single turnover reaction of heme-rHO-1 complex with wild-type CPR (Fig. 3*A*). The heme complexed with rHO-1 changed immediately to the ferrous oxy form, as indicated by the appearance of the 539- and 576-nm peaks, upon the addition of NADPH (25 μM, 5 eq to heme-rHO-1 complex) and the wild-type CPR (0.04 μM). The ferrous oxy form was then transformed to biliverdin as indicated by the decrease in the Soret band and the increase in absorption around 680 nm. The heme bound to rHO-1 was completely degraded to biliverdin within 30 min under these conditions.

The effect of the NADPH/FMN-depleted CPR system on the absorption spectrum of the heme-rHO-1 complex is shown in

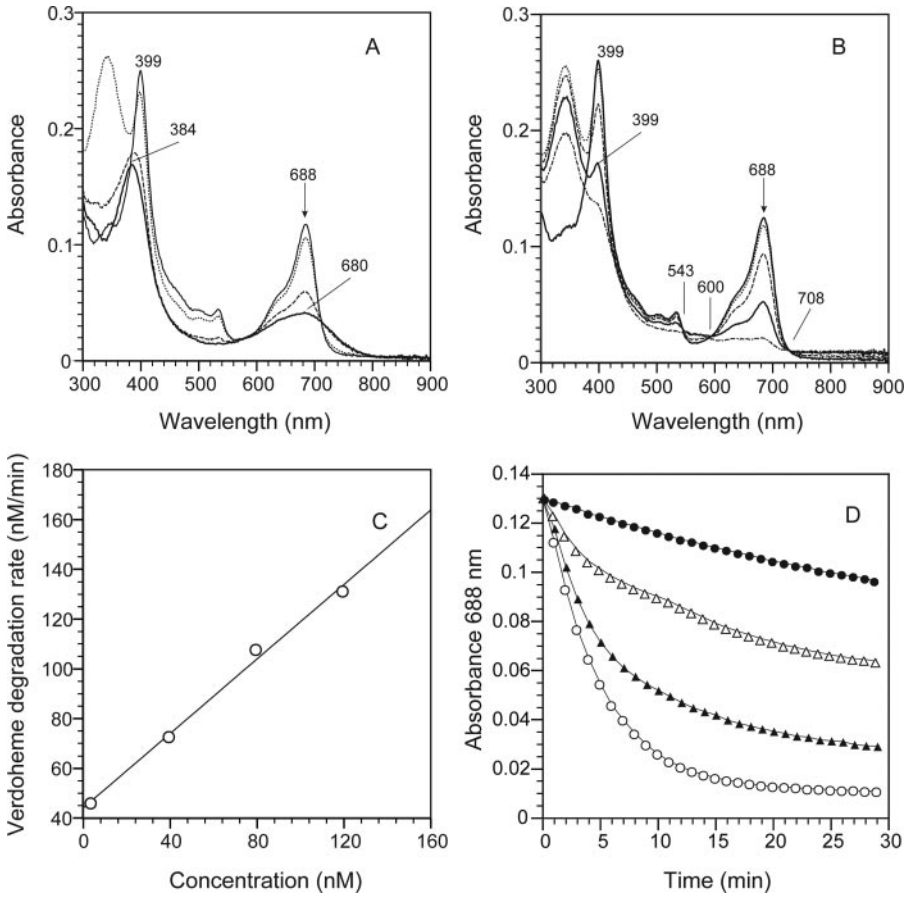

FIGURE 4. **Absorption spectral changes of the verdoheme-rHO-1 complex during the NADPH/CPR-supported single turnover reaction.** The spectra were recorded before (*thin solid line*) and after the addition of NADPH (*dotted line*, 1 min; *dashed line*, 10 min; *thick solid line*, 30 min; *dotted and dashed line*, 60 min). The procedures are described under "Experimental Procedures." *A*, with wild-type CPR; *B*, with FMN-depleted CPR. *C*, FMN-depleted CPR-dependent verdoheme degradation. The rate of degradation of verdoheme in complex with rHO-1 was calculated from the decrease of the absorbance at 399 nm. *D*, effect of ferricyanide on the FMN-depleted CPR-dependent degradation of verdoheme. Time-dependent absorbance changes at 688 nm were plotted in the reaction with 5 μM verdoheme-rHO-1 complex, 100 nM FMN-depleted CPR, 25 μM NADPH in the presence of 0 (*open circle*), 50 (*closed triangle*), 60 (*open triangle*), and 100 μM (*closed circle*) ferricyanide.

Fig. 3*B*. The addition of NADPH (25 μM) and the FMN-depleted CPR (0.04 μM) to the heme-rHO-1 complex did not cause any spectral changes except for an absorbance increase around 340 nm due to NADPH. Even with a 10-fold amount of the FMN-depleted CPR (0.4 μM), no spectral changes were observed (data not shown). Thus, it could be concluded that the first electron to reduce the ferric heme iron to the ferrous state must be transferred from FMN to HO.

Single Turnover Reactions of Verdoheme-rHO-1 Complex with NADPH/Wild-type and FMN-depleted CPR Systems—We next compared the degradation of verdoheme complexed with rHO-1 with wild-type and FMN-depleted CPR. Fig. 4*A* shows the changes in absorption spectra during the reaction of the verdoheme-rHO-1 complex with the NADPH/wild-type CPR system. Upon the addition of NADPH (25 μM) and wild-type CPR (0.04 μM), the 399-nm absorption peak of the verdoheme-rHO-1 complex decreased and shifted to 384 nm, and the intensity of the 688-nm peak decreased, leaving a broad absorption around 680 nm indicative of biliverdin formation. Thus verdoheme complexed with rHO-1 was completely degraded to biliverdin within 30 min under these conditions.

In contrast, upon the addition of the FMN-depleted CPR (0.04 μM) and NADPH (25 μM) to the verdoheme-rHO-1 complex, the 399- and 688-nm absorption peaks slowly decreased without any shift, and the absorbance between 800 and 900 nm increased (Fig. 4*B*). No additional spectral change was observed after 60 min, although about half of the NADPH still remained in the reaction mixture. The spectral changes showed three clear isosbestic points, at 543, 600, and 708 nm, indicating that no spectral intermediates are present in this reaction. The final spectrum bore a close resemblance to that of the ferric biliverdin-iron chelate reported previously (40). The rate of degradation of verdoheme in complex with rHO-1 was calculated from the decrease of the 399-nm absorbance of the verdoheme-rHO-1 complex (ϵ = 50.2 mM^{-1} cm^{-1}) and was found to be linearly dependent on the concentration of the FMN-depleted CPR (Fig. 4*C*).

That the product formed in the reaction with the FMN-depleted CPR is ferric biliverdin-iron chelate was confirmed by the addition of the ferric iron chelator desferrioxamine to the 60-min reaction mixture (Fig. 5*A*). The absorbance between 800 and 900 nm was decreased, and the 384-nm absorption peak and the broad band around 670 nm appeared with well defined isosbestic points at 585 and 750 nm, indicative of free biliverdin formation. When the wild-type CPR (0.04 μM) was added to the 60-min reaction mixture, the spectral changes observed were identical to those with desferrioxamine (Fig. 5*B*). Furthermore, we investigated the effect of ferricyanide on the rate of degradation of verdoheme in complex with rHO-1 with the NADPH/FMN-depleted CPR system. Fig. 4*D* shows the time-dependent absorbance changes at 688 nm of the verdoheme-rHO-1 complex, clearly indicating that the verdoheme degradation was inhibited by ferricyanide.

A somewhat worrying possibility is that the FMN-deleted CPR may generate a relatively larger amount of H_2O_2 compared with wild-type CPR, leading to accelerated conversion of verdoheme to biliverdin-iron chelate. Indeed, Matsui *et al.* (12) reported that H_2O_2 is an alternative and more efficient oxygen source than O_2 for verdoheme degradation to biliverdin under anaerobic conditions. In our aerobic reaction conditions with wild-type CPR or the FMN-depleted CPR and NADPH, the amount of H_2O_2 generated was at most 1 μM over a 60-min incubation (supplemental Table S2). Further, aerobic incuba-

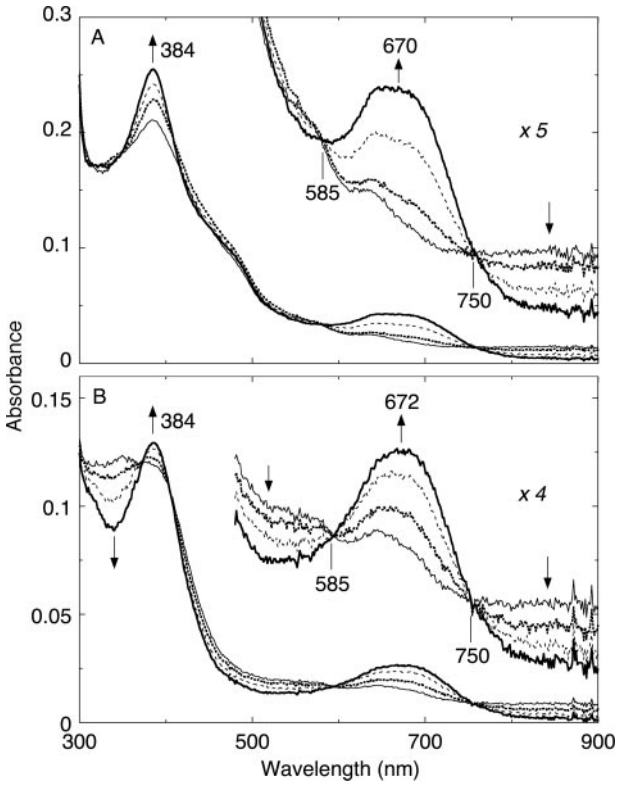

FIGURE 5. **Absorption spectral changes of the ferric biliverdin-iron chelate complex of rHO-1 during the NADPH/CPR-supported single turnover reaction.** The verdoheme-rHO-1 complex (5 μM) was incubated with NADPH (25 μM) and FMN-depleted CPR (0.08 μM). After 60 min, desferrioxamine (2 mM) (*A*) or wild-type CPR (0.04 μM) (*B*) was added to the mixture. Spectra before (*thin solid line*) and after the addition of desferrioxamine or wild-type CPR (*dotted line*, 1 min; *dashed line*, 10 min; *thick solid line*, 30 min) were monitored.

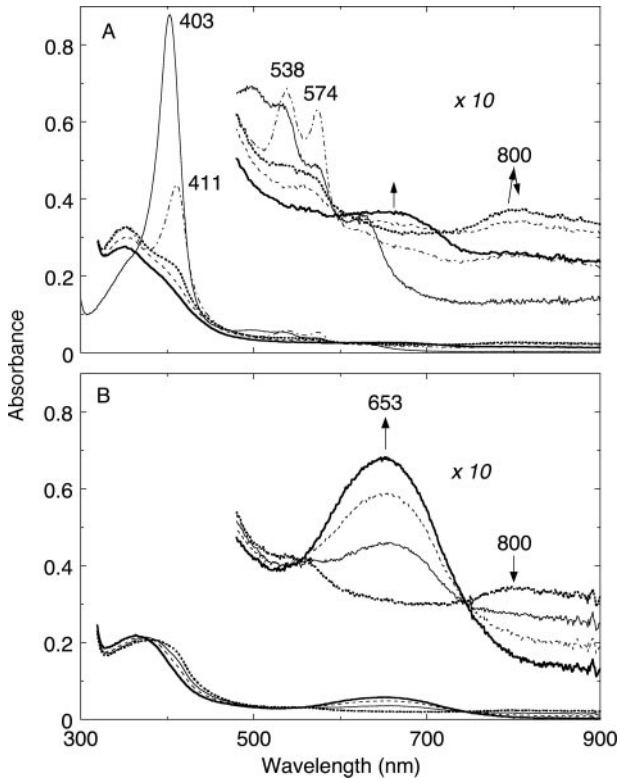

FIGURE 6. **Absorption spectral changes of FePPDME-rHO-1 complex during the ascorbate-supported single turnover reaction.** *A*, the spectra were recorded before (*thin solid line*) and after the addition of 20 mM ascorbate (*dotted and dashed line*, 1 min; *dotted line*, 9 min; *dashed line*, 39 min; *thick solid line*, 139 min) to the solution of FePPDME-rHO-1 complex (~5 μM) in 0.1 M potassium phosphate buffer (pH 7.4). *B*, desferrioxamine was added to the reaction mixture at 20 min after the addition of ascorbate. Spectra before (*dotted line*) and after the addition of desferrioxamine (*thin solid line*, 3 min; *dashed line*, 9 min; *thick solid line*, 39 min) were monitored.

tion of the verdoheme-rHO-1 complex with H_2O_2 (1 μM) caused nonproductive decomposition of verdoheme, not leading to biliverdin-iron chelate or biliverdin formation (supplemental Fig. S2), as reported previously (12).

These findings obtained with the FMN-depleted CPR indicate that electrons are certainly required for conversion of verdoheme to the ferric biliverdin-iron chelate and that they can be supplied by the FMN-depleted CPR without the involvement of FMN. The final electron, however, to reduce ferric biliverdin and release ferrous iron and biliverdin should be provided by FMN.

Single Turnover Reactions of the FePPDME-rHO-1 Complex—As mentioned above, the electrostatic interactions between the highly conserved basic residues, Lys^{179} and Arg^{183}, and the heme propionates are crucial not only for the proper accommodation of heme in the heme pocket but also for electron transfer between CPR and HO. To probe this, we constructed the FePPDME-rHO-1 complex and examined its single turnover reactions.

The optical spectra of the ferric, ferrous, and CO-bound forms of FePPDME-rHO-1 complex (supplemental Fig. S3) were very similar to those of the heme-rHO-1 complex (33), suggesting that the modifications of the heme propionate groups do not significantly affect the proximal histidine ligation and heme environment in the heme pocket.

First a single turnover reaction of the FePPDME-rHO-1 complex was carried out within the ascorbate-supported system. FePPDME complexed with rHO-1 decomposed to a species with a weak broad band around 800 nm (Fig. 6*A*). In order to confirm it as the iron chelate of biliverdin dimethyl ester, desferrioxamine was added to the reaction mixture 20 min after initiation. As shown in Fig. 6*B*, a broad absorption band appeared around 650 nm, indicative of formation of biliverdin dimethyl ester. The amount of biliverdin dimethyl ester was comparable with the amount of FePPDME-rHO-1 complex employed.

In a single turnover reaction of FePPDME-rHO-1 complex with the NADPH/wild-type CPR-supported system, the intensity of the Soret band decreased and red-shifted to 409 nm within 1 min and then further decreased with time (Fig. 7*A*). In the visible region, new absorption peaks at 537 and 573 nm corresponding to the oxy form of the FePPDME-rHO-1 complex appeared within 1 min, and they decreased along with the appearance of a new well resolved peak at 628 nm and a shoulder around 670 nm after 5 min. Thereafter, the absorbance in the 500–700-nm regions gradually decreased. With an excess of NADPH (200 μM), identical spectral changes were observed (data not shown). The addition of desferrioxamine to the reaction mixture 40 min after the reaction began produced a small broad absorption band around 650 nm, indicating that only a

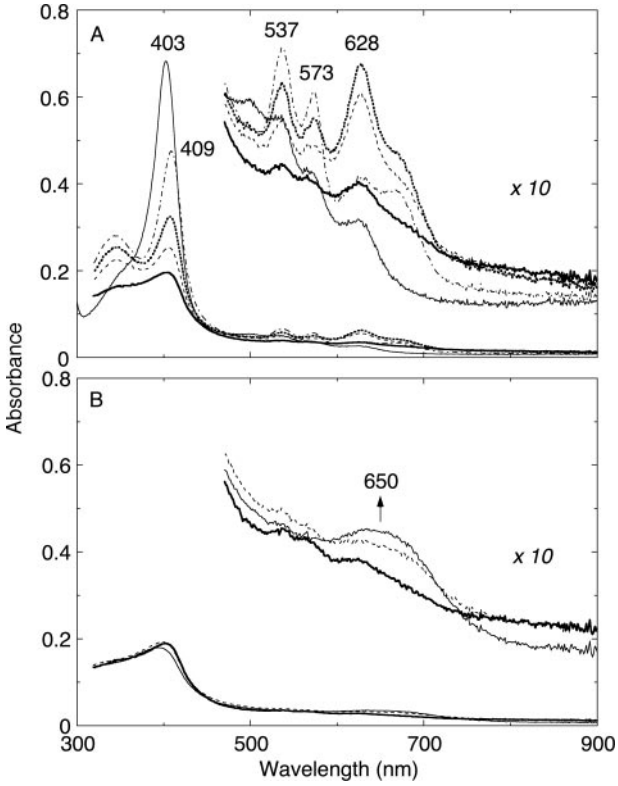

FIGURE 7. **Absorption spectral changes of FePPDME-rHO-1 complex during the NADPH/CPR-supported single turnover reaction.** *A*, the spectra were recorded before (*thin solid line*) and after the addition of NADPH (25 μM) (*dashed and dotted line*, 1 min; *dotted line*, 5 min; *dashed line*, 10 min; *thick solid line*, 25 min) to the solution of FePPDME-rHO-1 complex (~5 μM) and wild-type CPR (0.04 μM) in 0.1 M potassium phosphate buffer (pH 7.4). *B*, desferrioxamine was added to the reaction mixture at 40 min after the addition of NADPH. Spectra before (*thick solid line*) and after the addition of desferrioxamine (*dashed line*, 10 min; *thin solid line*, 40 min) were monitored.

part of the FePPDME-rHO-1 complex employed was converted to free biliverdin dimethyl ester in this system (Fig. 7*B*). The accumulated intermediate, showing a sharp peak at 628 nm with a shoulder around 670 nm was confirmed to be verdoheme dimethyl ester complexed with rHO-1 by repeating evacuation and flushing with N_2 gas and introducing CO (supplemental Fig. S4). The gradual decrease of the absorbance between 600 and 700 nm observed during the single turnover reaction of FePPDME-rHO-1 complex with the NADPH/wild-type CPR-supported system (Fig. 7*A*) was partly due to nonproductive decomposition of the verdoheme species by O_2 (8, 12).

HPLC analyses revealed that the biliverdin dimethyl esters produced in the single turnover reaction of the FePPDME-rHO-1 complex in the NADPH/wild-type CPR-supported reaction were 16.6 ± 3.5% biliverdin IXα dimethyl ester, 5.4 ± 0.5% IXβ, and 78.0 ± 3.8% IXδ, and in the ascorbate-supported reaction, they were 28.7 ± 3.2% biliverdin IXα dimethyl ester, 4.9 ± 0.9% IXβ, 1.2 ± 0.3% IXγ, and 65.2 ± 4.1% IXδ. The observed regioisomer ratios of biliverdin dimethyl ester in the NADPH/wild-type CPR- and ascorbate-supported reactions are similar to those found with the K18E/R183E double mutant of human HO-1 (30), in which the electrostatic interactions between Lys^{18} or Arg^{183} and heme propionates are probably weakened. Although the α-regiospecificity was lost in the FePPDME-rHO-1 complex, it should be noted that verdoheme dimethyl ester isomers accumulated in the CPR-supported reaction but not in the ascorbate-supported reaction.

DISCUSSION

In this study, we succeeded in preparing FMN-depleted CPR from the Y140A/Y178A mutant using the KBr method (35, 38). This depleted enzyme lost its ability to transfer an electron to cytochrome *c* but retained its ferricyanide-reducing activity (Tables 1 and 2). With the FMN-depleted CPR, we demonstrated that the degradation of heme in complex with rHO-1 never occurs (Fig. 4*B*), although the FMN-depleted CPR associates with the heme complex of rHO-1 with a binding affinity comparable with that of wild-type CPR. Thus, the first electron to reduce the ferric heme to the ferrous state in the HO-1 complex must be transferred from FMN. On the other hand, the FMN-depleted CPR is capable of serving as an electron donor to verdoheme in its complex with rHO-1, and indeed it is degraded to the ferric biliverdin-iron chelate in an FMN-depleted CPR-dependent manner (Fig. 4, *B* and *C*). Furthermore, this reaction is inhibited by the addition of ferricyanide (Fig. 4*D*), clearly indicating that electrons are required for conversion of verdoheme to the ferric biliverdin-iron chelate, and that they can be supplied by the FMN-depleted CPR through a pathway not involving FMN. This conclusion is also supported by the observation that verdoheme dimethyl esters are accumulated in the single turnover reaction of the FePPDME-rHO-1 complex in the NADPH/wild-type CPR system (Fig. 6*A*), although the methylation of heme propionates causes a loss of α-regiospecificity.

Ferric biliverdin-iron chelate, generated by the NADPH/FMN-depleted CPR system, was converted to biliverdin by the addition of the wild-type CPR or desferrioxamine (Fig. 5). Thus, the final electron for reducing ferric biliverdin-iron chelate to release ferrous iron and biliverdin is apparently provided by the FMN of CPR.

The most striking finding of the present study is that the electrons required for verdoheme oxidation can be supplied through an alternative pathway not involving FMN. It is reasonable to assume that the most probable electron-donating site in the FMN-deleted CPR is FAD. Indeed, it has been reported that partially FAD-deficient CPR shows a decreased ferricyanide reducing activity (36).

The HO reaction proceeds via a multistep mechanism that is different from other hemoproteins, such as cytochrome P450s and cytochrome b_5. The alternative electron pathway may function only for verdoheme degradation, which is considered to be a rate-limiting step of the HO reaction (12). However, whether or not this alternative pathway is available in wild-type CPR remains to be established. We believe that further analysis of the electron transfer pathway from CPR to HO-1 (*e.g.* employing FAD-depleted CPR) and the crystal structure of CPR-HO-1 complex should address this issue.

Recently, we (19) and the group of Ortiz de Montellano (41) have identified surface amino acids of HO-1 that are essential for binding to and/or electron transfer from CPR and have clarified some important interactions between those amino acid residues and CPR (Fig. 2). In our docking model of rat HO-1 and

rat CPR, there is a close contact between Lys^{149} in the distal F-helix of rHO-1 and the acidic cluster near the FMN site of CPR. In fact, a diminished reduction rate of ferric heme in complex with the rHO-1 mutants K149A or K153A has been observed (19). In addition, the distal F-helix of rHO-1 contains Asp^{140}, which participates in the hydrogen bonding network that provides protons required for the activation of O_2 bound to heme iron to hydroperoxide (30, 42). Our docking model also suggests that Arg^{185} of HO-1, the guanidino group of which could interact with 2′-phosphate of NADPH in CPR, is located two amino acid residues upstream from Arg^{183} that interacts electrostatically with the inner side heme propionate group in the heme-rHO-1 complex (20, 30).

It has been reported that substitutions of Asp^{140} in the distal heme pocket of rat and human HO-1 to Ala or Phe lead to destabilization of the distal hydrogen bonding network and completely abolish the first step of HO catalysis, the *meso*-hydroxylation of heme (42–44). Lad *et al.* (14) have reported the crystal structure of the ferrous verdoheme-human HO-1 complex, in which the water molecules, the constituents of the distal hydrogen bonding network, are missing. Consequently, in the crystal structure, the verdoheme can no longer interact with Asp^{140} through the hydrogen bonding network. However, in the crystal structure of rHO-1 containing the biliverdin-iron chelate, there is, in contrast to the structure of the verdoheme-human HO-1 complex, a hydrogen bonding network with Asp^{140}, including three water molecules (24). Thus, the conformation of the verdoheme-HO-1 complex surrounding verdoheme seems to be fairly distinct from those in the complexes of HO-1 with heme, α-hydroxyheme, or biliverdin-iron chelate (the crystal structure of α-hydroxyheme-HO-1 complex has yet to be determined). It is tempting to consider that the structural basis for the alternative electron transfer pathway may reside in the unique conformation of the verdoheme-HO-1 complex, but it should be noted that one of the propionate groups is also invisible in the crystal structure of the verdoheme-human HO-1 complex at 2.2 Å resolution (14). Its crystal structure at high resolution is awaited with great interest.

Ortiz de Montellano and co-workers (29, 30) have reported that with the Arg^{183} mutants of human HO-1, the rate of bilirubin formation in the presence of biliverdin reductase and ascorbate-supported system is little affected but that in the NADPH/CPR-supported system it is severely diminished. On the other hand, the double mutants, such as K18E/R183E, of human HO-1 showed a loss of α-regiospecificity, compared with the wild type in both NADPH/CPR- and ascorbate-supported systems. In addition, the hydrogen bonding network in the crystal structure of the heme-R183E HO-1 complex mutant has been found to be disordered (29). These facts as well as our findings obtained with FePPDME indicate that the heme propionate electrostatically interacting with Arg^{183} not only plays a role in properly orienting the heme but might also participate in electron transfer from FAD that occurs in the conversion of verdoheme to the biliverdin-iron chelate.

Acknowledgments—We thank Drs. Keiichi Fukuyama and Masakazu Sugishima for the helpful discussion on the docking model.

REFERENCES

1. Tenhunen, R., Marver, H. S., and Schmid, R. (1969) *J. Biol. Chem.* **244,** 6388–6394
2. Schacter, B. A., Nelson, E. B., Marver, H. S., and Masters, B. S. S. (1972) *J. Biol. Chem.* **247,** 3601–3607
3. Yoshida, T., Noguchi, M., and Kikuchi, G. (1980) *J. Biol. Chem.* **255,** 4418–4420
4. Ortiz de Montellano, P. R., and Auclair, K. (2003) in *Porphyrin Handbook* (Kadish, K., Smith K., and Guilard, R., eds) Vol. 12, pp. 183–210, Academic Press, Inc., New York
5. Ortiz de Montellano, P. R. (2000) *Curr. Opin. Chem. Biol.* **4,** 221–227
6. Yoshida, T., Noguchi, M., Kikuchi, G., and Sano, S. (1981) *J. Biochem.* (*Tokyo*) **90,** 125–131
7. Sakamoto, H., Omata, Y., Palmer, G., and Noguchi, M. (1999) *J. Biol. Chem.* **274,** 18196–18200
8. Sakamoto, H., Omata, Y., Hayashi, S., Harada, S., Palmer, G., and Noguchi, M. (2002) *Eur. J. Biochem.* **269,** 5231–5239
9. Yoshida, T., Noguchi, M., and Kikuchi, G. (1982) *J. Biol. Chem.* **257,** 9345–9348
10. Sakamoto, H., Omata, Y., Adachi, Y., Palmer, G., and Noguchi, M. (2000) *J. Inorg. Biochem.* **82,** 113–121
11. Sakamoto, H., Takahashi, K., Higashimoto, Y., Harada, S., Palmer, G., and Noguchi, M. (2005) *Biochem. Biophys. Res. Commun.* **338,** 578–583
12. Matsui, T., Nakajima, A., Fujii, H., Mansfield Matera, K., Migita, C. T., Yoshida, T., and Ikeda-Saito, M. (2005) *J. Biol. Chem.* **280,** 36833–36840
13. Liu, Y., and Ortiz de Montellano, P. R. (2000) *J. Biol. Chem.* **275,** 5297–5307
14. Lad, L., Ortiz de Montellano, P. R., and Poulos, T. L. (2004) *J. Inorg. Biochem.* **98,** 1686–1695
15. Strobel, H. W., Hodgson, A. V., and Shen, S. (1995) in *Cytochrome P450* (Ortiz de Moltellano, P. R., ed) pp. 225–244, Plenum Press, New York
16. Murataliev, M. B., Feyereisen, R., and Walker, F. A. (2004) *Biochim. Biophys. Acta* **1698,** 1–26
17. Iyanagi, T. (2005) *Biochem. Biophys. Res. Commun.* **338,** 520–528
18. Wang, M., Roberts, D. L., Paschke, R., Shea, T. M., Masters, B. S. S., and Kim, J. J. P. (1997) *Proc. Natl. Acad. Sci. U. S. A.* **94,** 8411–8416
19. Higashimoto, Y., Sakamoto, H., Hayashi, S., Sugishima, M., Fukuyama, K., Palmer, G., and Noguchi, M. (2005) *J. Biol. Chem.* **280,** 729–737
20. Sugishima, M., Sakamoto, H., Kakuta, Y., Omata, Y., Hayashi, S., Noguchi, M., and Fukuyama, K. (2002) *Biochemistry* **41,** 7293–7300
21. Lad, L., Schuller, D. J., Shimizu, H., Friedman, J., Li, H., Ortiz de Montellano, P. R., and Poulos, T. L. (2003) *J. Biol. Chem.* **278,** 7834–7843
22. Sugishima, M., Omata, Y., Kakuta, Y., Sakamoto, H., Noguchi, M., and Fukuyama, K. (2000) *FEBS Lett.* **471,** 61–66
23. Schuller, D. J., Wilks, A., Ortiz de Montellano, P. R., and Poulos, T. L. (1999) *Nat. Struct. Biol.* **6,** 860–867
24. Sugishima, M., Sakamoto, H., Higashimoto, Y., Noguchi, M., and Fukuyama, K. (2003) *J. Biol. Chem.* **278,** 32352–32358
25. Lad, L., Friedman, J., Li, H., Bhaskar, B., Ortiz de Montellano, P. R., and Poulos, T. L. (2004) *Biochemistry* **43,** 3793–3801
26. Sugishima, M., Sakamoto, H., Noguchi, M., and Fukuyama, K. (2003) *Biochemistry* **42,** 9898–9905
27. Frydman, R. B., Tomaro, M. L., Buldain, G., Awruch, J., Diaz, L., and Frydman, B. (1981) *Biochemistry* **20,** 5177–5182
28. Tomaro, M. L., Frydman, R. B., Frydman, B., Pandey, R. K., and Smith, K. M. (1984) *Biochim. Biophys. Acta* **791,** 342–349
29. Wang, J., Lad, L., Poulos, T. L., and Ortiz de Montellano, P. R. (2005) *J. Biol. Chem.* **280,** 2797–2806
30. Wang, J., Evans, J. P., Ogura, H., La Mar, G. N., and Ortiz de Montellano, P. R. (2006) *Biochemistry* **45,** 61–73
31. Zhou, H., Migita, C. T., Saito, M., Sun, D., Zhang, X., Ikeda-Saito, M., Fujii, H., and Yoshida, T. (2000) *J. Am. Chem. Soc.* **122,** 8311–8312
32. Omata, Y., Asada, S., Sakamoto, H., Fukuyama, K., and Noguchi, M. (1998) *Acta Crystallogr. Sect. D Biol. Crystallogr.* **54,** 1017–1019
33. Yoshida, T., and Kikuchi, G. (1979) *J. Biol. Chem.* **254,** 4487–4491
34. Hayashi, S., Omata, Y., Sakamoto, H., Hara, T., and Noguchi, M. (2003) *Protein Expression Purif.* **29,** 1–7

35. Vermilion, J. L., and Coon, M. J. (1978) *J. Biol. Chem.* **253,** 8812–8819
36. Kurzban, G. P., and Strobel, H. W. (1986) *J. Biol. Chem.* **261,** 7824–7830
37. Shen, A. L., Porter, T. D., Wilson, T. E., and Kasper, C. B. (1989) *J. Biol. Chem.* **264,** 7584–7589
38. Vermilion, J. L., and Coon, M. J. (1976) in *Flavins and Flavoproteins* (Singer, T. P., ed) pp. 674–678, Elsevier Scientific Publishing Co., Amsterdam
39. Iyanagi, T., and Mason, H. S. (1973) *Biochemistry* **12,** 2297–2308
40. Yoshida, T., and Kikuchi, G. (1978) *J. Biol. Chem.* **253,** 4230–4236
41. Wang, J., and Ortiz de Montellano, P. R. (2003) *J. Biol. Chem.* **278,** 20069–20076
42. Fujii, H., Zhang, X., Tomita, T., Ikeda-Saito, M., and Yoshida, T. (2001) *J. Am. Chem. Soc.* **123,** 6475–6484
43. Lightning, L. K., Huang, H., Moenne-Loccoz, P., Loehr, T. M., Schuller, D. J., Poulos, T. L., and Ortiz de Montellano, P. R. (2001) *J. Biol. Chem.* **276,** 10612–10619
44. Lad, L., Wang, J., Li, H., Friedman, J., Bhaskar, B., Ortiz de Montellano, P. R., and Poulos, T. L. (2003) *J. Mol. Biol.* **330,** 527–538

Supplemental data

1) CD spectra of wild-type and FMN-depleted CPR

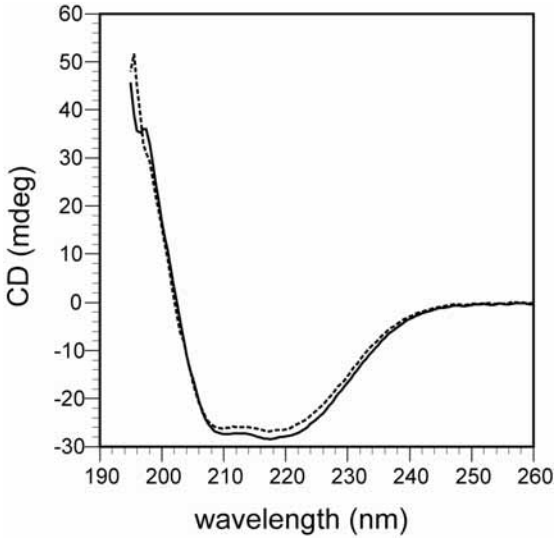

Fig. S1. CD spectra of wild-type (———) and FMN-depleted CPR (--------). The CD spectra were recorded on a JASCO J-815 spectropolarimeter using a 1-cm path length quartz cell. Protein concentrations were 25 μg/ml in 10 mM potassium phosphate buffer containing 1 mM EDTA, 0.1 mM dithiothreitol, pH 7.7. Data were collected from 260 to 195 nm at 0.5 nm intervals and at a rate of 100 nm/min with a response time of 2 s for each point. Spectra were presented as an average of eight repeats.

Table S1. Secondary structures of wild-type and FMN-depleted CPR

	secondary structure (%)[a]			
	α-helix	β-sheet	turn	random
wild-type CPR	36	17	18	29
FMN-depleted CPR	35	17	19	29

[a]The predicted contents of secondary structures were calculated using the SELCON3 program (S1)

2) H_2O_2-dependent verdoheme degradation

Table S2. Quantification of H_2O_2 produced by the NADPH/wild-type CPR and the NADPH/FMN-depleted CPR systems.

Enzyme	Incubation time	H_2O_2
	min	*μM* [a]
wild-type CPR	10	0.13
	30	0.63
	60	1.08
FMN-depleted CPR	10	0.14
	30	0.61
	60	1.06

[a]A solution of wild-type or FMN-depleted CPR (40 nM) in 0.1 M potassium phosphate buffer, pH 7.4 was incubated with 25 μM NADPH for the indicated period at room temperature in the air. Quantification of H_2O_2 was performed employing Bindschedler's Green method (S2). Briefly, 0.2 ml of test solution and 1.8 ml of color reagent solution containing 0.1 mM *N*-(carboxymethylaminocarbonyl)-4,4-bis (dimethylamino) diphenylamine sodium salt (Wako, Osaka, Japan), 0.1 mM PEPES, pH 7.0, 0.5 % Triton X-10 and 1U/ml horseradish peroxidase (Sigma, St. Louis, MO) were incubated for 5 min at 37 °C. The absorbance at 727 nm (ε = 90 $mM^{-1}cm^{-1}$) was measured.

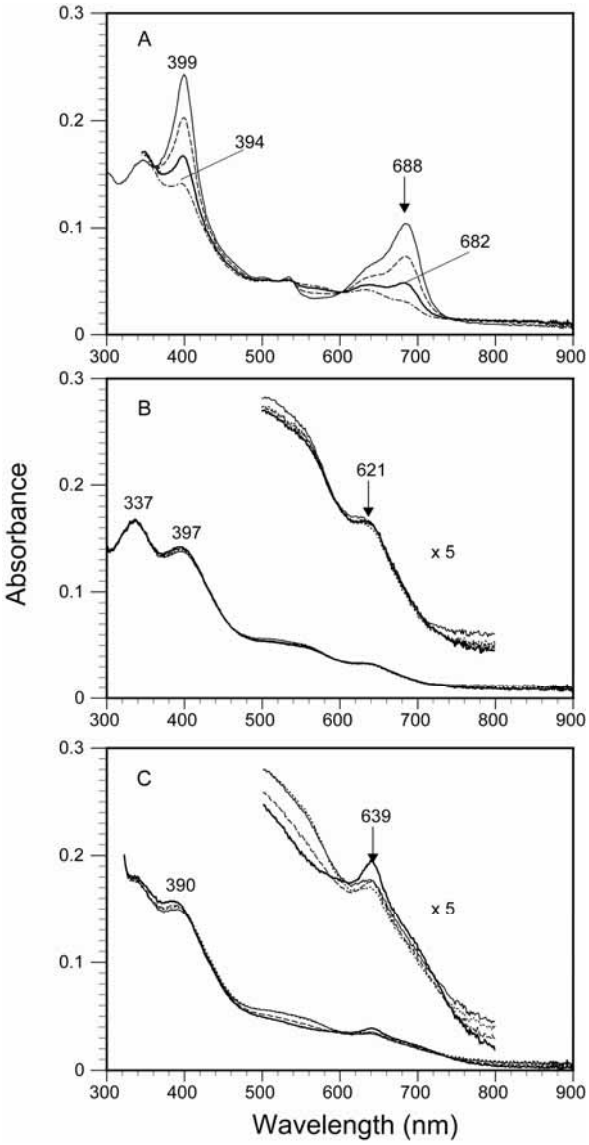

Fig. S2. Absorption spectral changes of the verdoheme–rHO-1 complex during the incubation with H_2O_2. *(A)* The spectra were recorded before (———) and after the addition of H_2O_2 (1 μM) (10 min, --------; 30 min, ▬▬▬; and 60 min, −·−·−·−) to the solution of verdoheme-rHO-1 complex (ca. 5 μM) in 0.1 M potassium phosphate buffer (pH 7.4). After 60 min, *(B)* desferrioxamine (2 mM) or *(C)* ascorbate (20 mM) was added to the mixture. Spectra before (———) and after the addition of desferrioxamine or ascorbate (1 min, ·····; 10 min, --------; 30 min, ▬▬▬) were monitored.

3) Degradation of FePPDME in complex with rHO-1

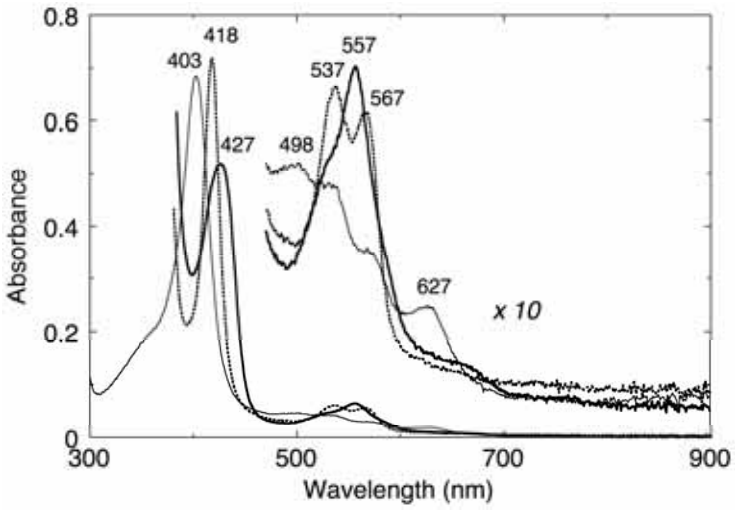

Fig. S3. Optical absorption spectra of FePPDME-rHO-1 complex (ca. 5 μM) in ferric (———), ferrous (▬▬▬) and CO-ferrous (·····) forms in 0.1 M potassium phosphate buffer (pH 7.4). Its ferrous complex was formed by reduction of the ferric complex with a few grains of sodium dithionite and its ferrous carbon monoxide complex was formed by saturating the ferric complex solution with CO gas by bubbling for 1 min followed by reduction with a few grains of sodium dithionite.

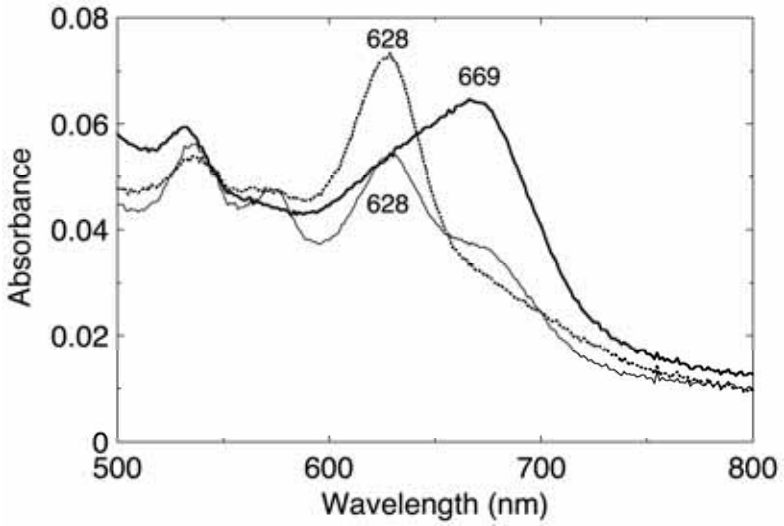

Fig. S4. Spectroscopic characterization of the accumulated intermediates in the NADPH/CPR-supported single turnover reaction of FePPDME-rHO-1 complex. Reaction conditions were the same as those shown in Fig. 7. *Solid line(———):* The intermediate accumulated during first 5 min; *Bold line(━━━━):* After replacing the gas phase with N_2 gas; *Dotted line(·····):* After the introduction of CO.

Additional caption to Fig. S4- The intermediate accumulated, showing a sharp peak at 628 nm with a shoulder around 670 nm was confirmed to be verdoheme dimethyl ester in complex with rHO-1. By repeating evacuation and flushing with N_2 gas, the sharp peak at 628 nm was decreased and the shoulder was increased to show a clear peak at 669 nm. When CO gas was introduced into the cuvette, the peak at 669 nm was decreased and the 628-nm peak was increased again. Thus it was concluded that the 628- and 670-nm species are CO-ferrous and ferrous forms of verdoheme dimethyl ester, respectively.

References for supplemental data

S1. Sreerama, N, and Woody, R. W. (1993) *Anal. Biochem*. **209**, 32-44

S2. Takagi, K., Tatsumi, Y., Kitaichi, K., Iwase, M., Shibata, E., Nakao, M., Matsumoto, T., Takagi, K., and Hasegawa, T. (2004) *Clin. Chim. Acta* **340**, 219-227

The Reactions of Heme- and Verdoheme-Heme Oxygenase-1 Complexes with FMN-depleted NADPH-cytochrome P450 Reductase: ELECTRONS REQUIRED FOR VERDOHEME OXIDATION CAN BE TRANSFERRED THROUGH A PATHWAY NOT INVOLVING FMN

Yuichiro Higashimoto, Hideaki Sato, Hiroshi Sakamoto, Kenichi Takahashi, Graham Palmer and Masato Noguchi

J. Biol. Chem. 2006, 281:31659-31667.
doi: 10.1074/jbc.M606163200 originally published online August 22, 2006
